

Micro/Nanostructured Papers from Bagasse Pulp Reinforced by Nanofibrillated Cellulose from different Agro-Waste Sources

Nattakan Soykeabkaew^{1, 2*}, Phattharasaya Rattanawongkun¹, Nuchanad Kunfong¹, Supattra Klayya¹, Nattaya Tawichai^{1, 2}, Uraivan Intatha^{1, 2}

¹School of Science, Mae Fah Luang University, 333 M 1, Muang, Chiang Rai, 57100, Thailand

²Center of Innovative Materials for Sustainability (iMatS), Mae Fah Luang University, Chiang Rai, 57100, Thailand

*Corresponding author: E-mail: nattakan@mfu.ac.th; Tel: (+66) 5391 6774

Received: 25 February 2019, Revised: 11 March 2019 and Accepted: 29 April 2019

DOI: 10.5185/amlett.2019.0011

www.vbripress.com/aml

Abstract

The nanofibrillated celluloses (NFCs) from banana pseudostem (BA) and pineapple leaf (PA) were prepared by soda pulping pretreatment and microfluidization. TEM and XRD results revealed a slight diverse in features of both NFCs. Their average diameter was 15.5-20.0 nm with ~1.7 μm average length. Each NFC (1-5 wt%) was integrated into the bagasse microfiber (BG) papers. From SEM images, it was showed that the voids between the microfibrils were filled up and bridged by NFCs, hence, greatly increasing fiber bonded area and remarkably reinforcing the papers as a result. The BG/NFC-BA 5 wt% sheet exhibited to be the strongest one. Then again, the BG/NFC-PA 5 wt% sheet (highly elongated before breaking) was shown to be the toughest one. This can bring a conclusion that NFCs can effectively be used to improve quality of the microfiber papers in many aspects. In addition, it was also found that the source of NFCs showed a noticeable influence on the paper strength while the quantity of added NFCs was more critical to the paper toughness. Therefore, a selection of both suitable source and usage quantity of NFCs for desired performance of papers and other related products has to be considered beforehand. Copyright © VBRI Press.

Keywords: Micro/nanostructured materials, bagasse, paper, nanofibrillated cellulose, agro-waste.

Introduction

During the last decade, the production and consumption of paper and its related products continuously increased [1]. Due to a finite supply capacity of forest cellulosic materials, the resources saving strategies by decreasing basis weight of paper products as well as strengthening them are essential [2]. In previous researches, nanocelluloses or cellulose nanofibers have demonstrated to be a highly promising reinforcement in pulp and paper applications [3-10] owing to their attractive characters such as high specific surface, high aspect ratio, high intrinsic mechanical properties, renewability, sustainability, abundance, biodegradability, and capacity to be functionalized in numerous ways. Cellulose nanofibers can be extracted from both wood and non-wood resources. Thus, underutilized agro-wastes can also be considered as a valuable raw material to produce nanocelluloses [11]. Various agro-wastes such as bagasse [4], maize stalk [5], wheat straw [11], and palm rachis [12] were recently studied for isolation of nanocelluloses. Typically, cellulose nanofibers can be classified by their dimensions, functions, and preparation methods. According to their dimensions, cellulose nanofibers are

subdivided into cellulose nanocrystal (CNC) and nanofibrillated cellulose (NFC). CNC exhibits crystalline rod-like shapes (from plant sources) with diameter and length of around 5-70 nm and 100-250 nm, respectively. It has very low degree of flexibility compared to NFC because it does not contain amorphous region. On the other hand, NFC are often referred to as spaghetti-like, with diameter of around 5-60 nm and length of several micrometers. It is consisted of both the crystalline and amorphous regions, long, entangled, and flexible [9, 10, 13]. Owing to its longer length with good flexibility, NFC puts forward a high potential to interact with pulp cellulosic fibers through hydrogen bonding as well as create a strong entangled network accounted which can effectively contribute to an improvement in paper quality [9].

In this study, NFCs were prepared from two agro-waste sources, *i.e.* pineapple leaf (PA) and banana pseudostem (BA), and then used to reinforce in the bagasse microfiber (BG) papers which were formed by hot-pressing. Characteristic, morphology, structure, physical and mechanical properties of the NFCs and micro/nanostructured papers (both BG/NFC-BA and BG/NFC-PA papers) were investigated using TEM, XRD, SEM, density measurement, and tensile testing.

Experimental

Materials

The cultivated banana pseudostem (BA) from the Botanical Garden of Mae Fah Luang University and pineapple leaves (PA) from Nang Lae area, Chiang Rai, Thailand were used as raw materials to prepare NFCs in this study. At first, they were dried and grounded into small pieces by pulverizer before further treatments. The bagasse (BG) sheet was supplied by our project partner: the Biodegradable Packaging for Environment Public Co., Ltd., Chainat, Thailand. Sodium hydroxide (NaOH) pellets were purchased from QR&C, New Zealand.

Nanofibrillated Celluloses (NFCs) preparation

Firstly, the pulp was extracted from the dried BA and PA by a soda pulping process. In this step, the BA and PA were treated with 18 wt% NaOH solution and the liquid:solid ratio of 10:1 at $98 \pm 2^\circ\text{C}$ for 30 min. The obtained pulps were then washed by tap water to remove the unreacted chemical reagent and black liquor until cleaned and neutralized. Afterward, the pulps were disintegrated by using a kitchen blender (House Worth model HW-BDC2PC) at 15,000 rpm for 1 min before screening. The collected pulps for further use were the screened portion between the two metal meshes no. 18 and 200 with opening sieve sizes of 1 mm and 74 μm , respectively. Next, to prepare NFCs, the pulp fibers were diluted to 0.5% consistency and defibrillated the fibers through the interaction chamber of 87 μm of a lab-scale M-110P Microfluidizer (Microfluidics Corporation, USA) at 25,000 psi for 20 passes.

Preparation of micro/nanostructured papers

The received BG sheet was torn into small pieces (ca. 1 cm \times 1 cm) and soaked in tap water overnight before disintegrated into pulp suspension by using the kitchen blender at 15,000 rpm for 5 min. Then, the pulp was screened by the two metal meshes no. 18 and 200 and the screened portion of BG fibers was adjusted to 2% consistency before mixing with the NFC-BA or NFC-PA. In this step, each NFC slurry was added to the BG suspension at loading content of 1 and 5 wt% (based on dried weight of BG) and then mixed for 1 min by stirring. Next, the mixture was partially dewatered by hand pressing between the two metal meshes no. 400 and subsequently compressed and molded (Scientific LP-S-80, Labtech Engineering, Thailand) into a paper sheet at 105°C under pressure of 159 kPa for 5 min. The pure BG sheet without NFC addition was also formed for comparison purpose. The grammage of all paper sheets made were to be in the range of 224-294 g/m^2 .

Characterization, measurement and testing

The NFC characteristics were analyzed using a TEM (Hitachi HT7700, Japan) at an accelerating voltage of 80 kV. Each NFC slurry was diluted to 0.001% consistency and then dropped on a copper grid with

formvar film support. The droplet was maintained on the grid for 5 min, before strained with a 2% aqueous uranyl acetate, and kept overnight before the examination. The NFC dimensions were measured and reported from the average of 10 fibers. On the other hand, the BG dimension was measured from several SEM images. The reported values were averaged from 50 fibers. The SEM images of BG fibers, surfaces and fractured surfaces (after the tensile test) of the paper sheets were taken by using an SEM (LEO 1450 VP, USA) at an accelerating voltage of 10 kV. A thin layer of gold was sputtered and coated on the samples prior to the investigation.

Crystallinity Index (CrI) of the NFCs was examined through XRD using a Philips X'pertPro MPD. The NFC sheets were casted and then irradiated by Cu-K α radiation operated at 40 kV and 30 mA. XRD patterns were recorded from 10° - 30° (2θ) at a scan speed of $2^\circ/\text{min}$. Segal's method was used to calculate CrI of each NFC sample according to the following equation:

$$\text{CrI} (\%) = [(I_{002} - I_{\text{am}}) / I_{002}] \times 100 \quad (1)$$

where I_{002} is the intensity of the cellulose II crystal reflection at $2\theta = 21.9^\circ$ and I_{am} is the intensity of the amorphous scatter at $2\theta = 18^\circ$ [14, 15].

To measure the density of the paper sheets, they were cut into rectangular specimens (10 mm \times 50 mm) and weighted (g). Then, the thickness, width and length of each specimen were determined using digital calipers and averaged from at least 3 replicates per specimen. The specimen dimension was used for the calculation of each specimen's volume (cm^3). The density (ρ) of the specimens was later calculated according to the ratio of its weight to volume (g/cm^3). The grammage of the papers (g/m^2) as defined by weight (g) per unit area (m^2) (according to TAPPI T410) was as well calculated and reported. Also, the porosity of each specimen was estimated by using the following equation:

$$\text{Porosity} (\%) = [1 - (\rho_{\text{paper}} / \rho_{\text{cellulose}})] \times 100 \quad (2)$$

where the density of cellulose is $1.592 \text{ g}/\text{cm}^3$ [15].

Tensile testing of the paper sheets was carried out using an Instron machine (model 5566, USA) equipped with a 1 kN load cell. The width and gauge length of specimens were 10 mm and 30 mm, respectively. All specimens were conditioned at 50% relative humidity (RH) at 25°C overnight before testing. The constant cross-head speed of 15 mm/min and pre-load of 1 N were set for the test. The tensile index, tensile strength, elongation, toughness (assessing from area under stress-strain curve), and Young's modulus of the paper specimens were evaluated subsequently and the reported values were obtained from the average of 5 tested specimens.

Results and discussion

TEM images of the obtained NFC-BA and NFC-PA after 5, 10, and 20 passes through the microfluidizer are shown

in **Fig. 1a-c** and **Fig. 1d-f**, respectively. It showed that the products were defibrillated to higher degrees with increasing number of passes and changed from web-like network into more individual nanofibrils with clear head and tail, particularly after 20 passes. Therefore, the NFCs with 20 passes were selected for the further study. The average diameter and length of both NFC-BA and NFC-PA were found to be very close, around 15-20 nm and 1.7 μm , respectively.

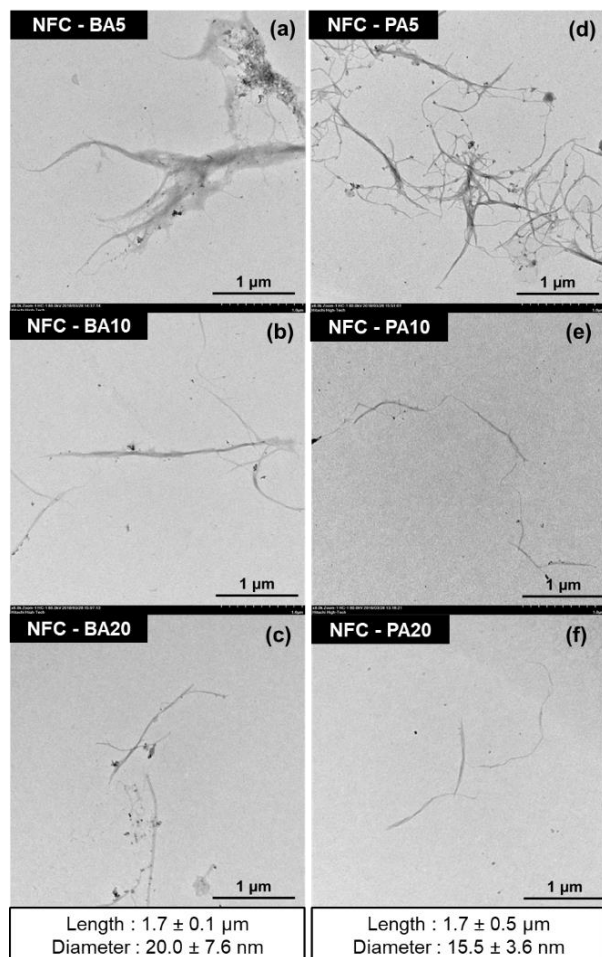


Fig. 1. TEM photographs of NFC-BA (a-c) and NFC-PA (d-f) showing the change in NFC feature from web-like network into more individual nanofibrils after 5, 10, and 20 passes through a microfluidizer.

The XRD patterns of both NFCs are presented in **Fig. 2**. From the peaks, the presence of type II cellulose in the NFCs was indicated by the reflection at $2\theta = 12.0^\circ$, 20.0° , and 21.9° which was assigned to the crystallographic planes of $(\bar{1}10)$, (110) , and (020) of cellulose II [16]. Thus, after the soda pulping and microfluidization of BA and PA, the transformation of native cellulose from cellulose I to cellulose II was occurred. The crystallinity index (CrI) of NFC-BA and NFC-PA was 61% and 69%, respectively.

From TEM and XRD results, it suggested that characteristics of the NFC products from different agro-wastes could be very similar if they were passed through the same pretreatment and nanocellulose isolation method.

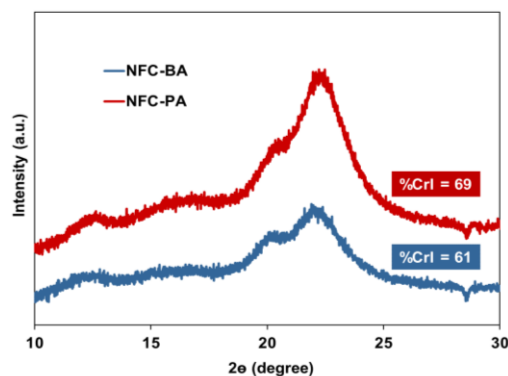


Fig. 2. XRD patterns of NFC-BA and NFC-PA indicating the transformation of native cellulose I (in BA and PA) to cellulose II polymorph after the soda pulping pretreatment and NFC mechanical isolation.

Fig. 3 shows the SEM micrographs of surface morphology of the pure BG paper (**Fig. 3a**) and micro/nano papers of BG/NFCs. With NFC addition, the voids between BG microfibrils were seen to be shallower and fewer (see **Fig. 3b** and **3c**). This indicated that NFCs helped in filling up these voids as well as merging the BG fibers together. In agreement with the data of measured density of these papers, it was significantly increased (15.3 - 21.3%) with 5 wt% NFC addition (see **Table 1**). The porosity of the micro/nano papers was also greatly decreased (18.4 - 25.7%) when compared to that of the pure BG paper.

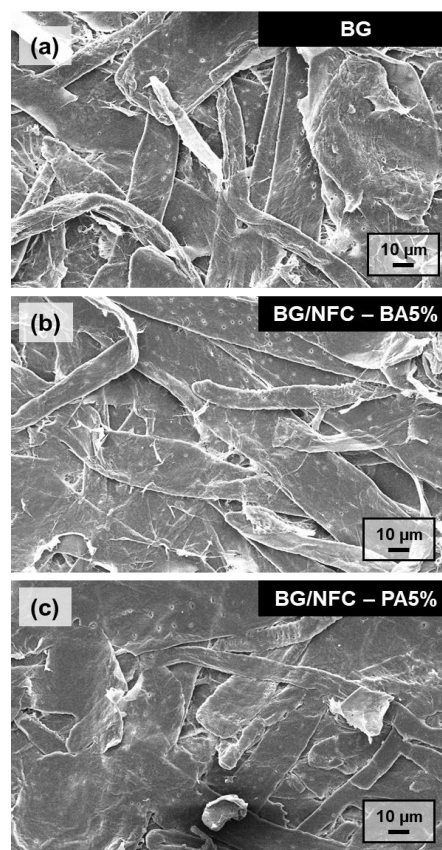
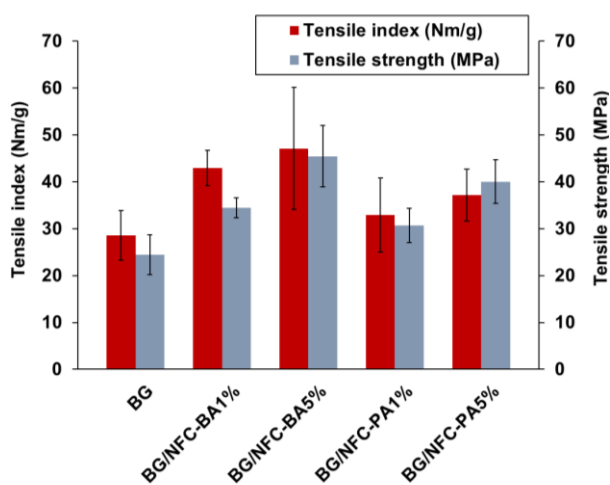


Fig. 3. SEM micrographs of surfaces of the BG papers reinforced with NFCs at different contents. (a) 0 wt%; (b) NFC-BA 5 wt%; (c) NFC-PA 5 wt%.

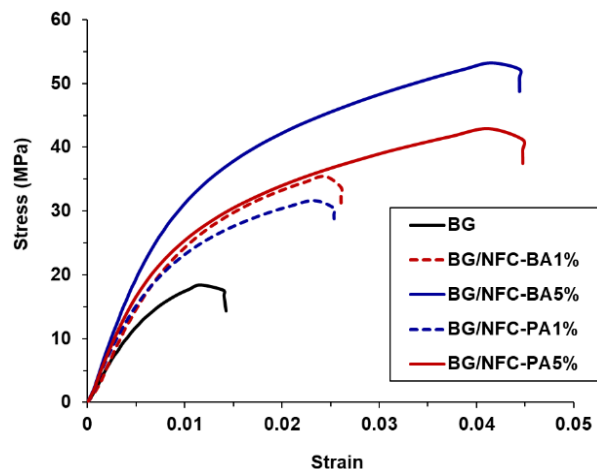
Table 1. The measured density and porosity of the BG and micro/nanostructured papers.

Sample	Density (g/cm ³)	Porosity (%)
BG	0.87	45.31
BG/NFC-BA 1%	0.89	44.30
BG/NFC-BA 5%	1.00	36.97
BG/NFC-PA 1%	1.03	35.42
BG/NFC-PA 5%	1.06	33.65

From the tensile testing results, the strengthening effect of both NFCs on the BG papers was shown to be remarkable. Only 1 wt% NFC-BA could increase both the tensile index (N.m/g) and tensile strength (MPa) of the papers by 50.2% and 41.2%, respectively (Fig. 4).

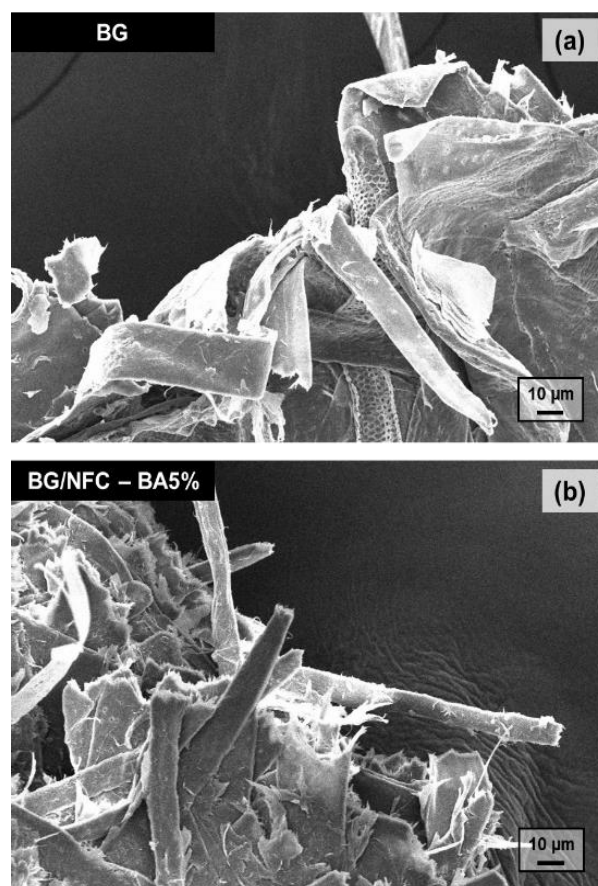
**Fig. 4.** Strengthening effect of NFCs on the tensile index and strength of the micro/nanostructured papers.

The higher amount (5 wt%) of NFCs further enhanced the tensile properties of the papers. The elongation at break (%) of the BG/NFC-PA5% paper was found to increase up to 140%. Furthermore, after integrating the area under its stress-strain curve (plotting in Fig. 5), the toughness (MJ/m³) or energy needed to brake the sample was almost 4-fold increase (see Table 2).

**Fig. 5.** Stress-strain curves of the pure BG and BG papers with integration of different NFCs at 1 wt% and 5 wt% loading content.**Table 2.** The elongation at break and toughness of the sample papers assessed from the tensile test.

Sample	Elongation (%)	Toughness (MJ/m ³)
BG	1.55 ± 0.38	0.25 ± 0.10
BG/NFC-BA 1%	2.69 ± 0.41	0.72 ± 0.23
BG/NFC-BA 5%	3.53 ± 1.16	1.02 ± 0.48
BG/NFC-PA 1%	2.00 ± 0.29	0.51 ± 0.10
BG/NFC-PA 5%	3.72 ± 0.49	1.18 ± 0.30

SEM images of the failed samples (Fig. 6) also indicated changes in failure mode of this paper in the presence of NFCs. The stretching and yielding of fibers along with the applied load direction were allowed before breaking as revealed in the fractured surface of the micro/nanostructured paper (Fig. 6b). All, thanks to the nano-size effect of NFCs for an escalation in connectivity within BG fibers, fiber-fiber bonding, and bonded area [4, 5, 9] through filling voids and bridging adjacent microfibrils as previously confirmed by SEM (see Fig. 3).

**Fig. 6.** SEM micrographs of fractured surfaces of (a) the pure BG and (b) BG/NFC-BA 5 wt% papers.

Additionally, the earlier discussion seemed to propose that advances in the tensile properties of the micro/nanostructured papers prominently depended on both NFC's type and amount. For the paper strength, the NFC type was shown to be more influential. However, the amount of added NFCs appeared to be more critical for a pronounced increase in the paper toughness.

Conclusion

NFCs from the two agro-wastes (i.e., banana pseudostem and pineapple leaf) were prepared by the soda pulping pretreatment and then passing through a microfluidizer for up to 20 cycles. By using the same pretreatment and nanocellulose isolation process, NFC products from different sources were shown to be slightly differ in their characteristics (e.g., dimension and crystalline structure) investigated by TEM and XRD. When this NFCs were integrated into the BG microfibers, the density of the BG/NFC papers was visibly increased while their porosity was decreased. SEM results revealed that NFCs caused fewer and shallower voids remained in the paper structures by filling them up and merging the microfibers together. This increased connectivity, interfiber bonding and bonded area led to a markedly improvement in all tensile performances of the present micro/nano-structured papers. Type of NFCs was shown to have a pronounced influence on the paper strength. On the other hand, the loading content of NFCs was found to be more prominent on the paper toughness. Towards the end, this study suggests that the resources saving strategy by decreasing basis weight of paper products is highly promising thank to the remarkably reinforcing effect of NFCs. However, more effort and development to lower energy and time consumption in the NFCs production are crucially required so that cheaper NFCs can then be widely available. If not, using NFCs as only a reinforcement in paper and its related products could vastly increase the cost and might not be worth it. In addition, for real uses and novel applications of these micro/nanostructured papers, other related properties, characteristics, production cost, etc. are needed to be further assessed and considered.

Acknowledgements

The joint funding support (grant code 256101A3070019) from the National Research Council of Thailand (NRCT) and National Science Technology and Innovation Policy Office (STI) is gratefully acknowledged. Without supports and facilities from our industrial partner, the Biodegradable Packaging for Environment Public Co., Ltd. (Gracz) as well as Mae Fah Luang University (MFU) and the PLC Holding Co., Ltd., Thailand, this research would have not been succeeded. Thank you.

Author's contributions

Conceived the plan: N.S., N.T., U.I.; Performed the experiments: P.R., N.K., S.K.; Data analysis: N.S., P.R., N.K., S.K.; Wrote the paper: N.S. Authors have no competing financial interests.

Conflicts of interest

There are no conflicts to declare.

References

1. Tarrés, Q.; Pellicer, N.; Balea, A.; Merayo, N.; Negro, C.; Blanco, A.; Delgado-Aguilar, M.; Mutjé, P.; *Int. J. Biol. Macromol.*, **2017**, *105*, 664.
2. Tarrés, Q.; Oliver-Ortega, H.; Alcalà, M.; Merayo, N.; Balea, A.; Blanco, A.; Mutjé, P.; Delgado-Aguilar, M.; *Carbohydr Polym.*, **2018**, *183*, 201.
3. González, I.; Boufi, S.; Pèlach, M.A.; Alcalà, M.; Vilaseca, F.; Mutjé, P.; *Bioresources*, **2012**, *7*, 5167.
4. Afra, E.; Yousefi, H.; Hadilam, M.M.; Nishino, T.; *Carbohydr Polym.*, **2013**, *97*, 725.
5. Mtibe, A.; Liganiso, L.Z.; Mathew, A.P.; Oksman, K.; John, M.J.; Anandjiwala, R.D.; *Carbohydr Polym.*, **2015**, *118*, 1.
6. Rantanen, J.; Dimic-Misic, K.; Kuusisto, J.; Maloney, T.C.; *Cellulose*, **2015**, *22*, 4003.
7. Balea, A.; Blanco, A.; Monte, M.C.; Merayo, N.; Negro, C.; *BioResources*, **2016**, *11*, 8123.
8. Abdul Khalil, H.P.S.; Davoudpour, Y.; Saurabh, C.K.; Hossain, M.S.; Adnan, A.S.; Dungani, R.; Paridah, M.T.; Sarker, M.Z.I.; Fazita, M.R.N.; Syakir, M.I.; Haafiz, M.K.H.; *Renew Sust Energ Rev.*, **2016**, *64*, 823.
9. Boufi, S.; González, I.; Delgado-Aguilar, M.; Tarrès, Q.; Pèlach, M.A.; Mutjé, P.; *Carbohydr Polym.*, **2016**, *154*, 151.
10. Osong, S.H.; Norgren, S.; Engstrand, P.; *Cellulose*, **2016**, *23*, 93.
11. Zimmermann, T.; Bordeanu, N.; Strub, E.; *Carbohydr Polym.*, **2010**, *79*, 1086.
12. Hassan, M.L.; Bras, J.; Mauret, E.; Fadel, S.M.; Hassan, E.A.; El-Wakil, N.A.; *Ind Crops Prod.*, **2015**, *64*, 9.
13. Khalil, H.P.S.A.; Davoudpour, Y.; Islam, M.N.; Mustapha, A.; Sudesh, K.; Dungani, R.; Jawaid, M.; *Carbohydr Polym.*, **2014**, *99*, 649.
14. Park, S.; Baker, J.O.; Himmel, M.E.; Parilla, P.A.; Johnson, D.K.; *Biotechnol Biofuels.*, **2010**, *3*, 10.
15. Tabarsa, T.; Sheykhazari, S.; Ashori, A.; Mashkour, M.; Khazaiean, A.; *Int. J. Biol. Macromol.*, **2017**, *101*, 334.
16. Chen, Y.W.; Lee, H.V.; *Int. J. Biol. Macromol.*, **2018**, *107*, 78.